Solution Mining Research Institute; Fall 2005 Technical Meeting

Nancy, France, October 2-5, 2005

BEHAVIOR INTERPRETATION OF MECHANICAL INTEGRITY TESTS

Mehdi Karimi-Jafari[1], Leo Van Sambeek[2], Benoît Brouard[3], Pierre Bérest[1], Behrouz Bazargan[4]

[1]LMS, Ecole Polytechnique, 91128 Palaiseau France
[2]RESPEC, P.O. Box 725 Rapid City, South Dakota 57709 USA
[3]Brouard Consulting, 101 rue du Temple 75003 Paris France
[4] Bureau de Recherches Géologiques et Minières, Orléans, France

Introduction

Interpretation of tightness tests in underground salt caverns is the main concern of this paper. Much of the material used to prepare this paper was first included in a report prepared for the SMRI (Van Sambeek *et al*., 2005).

Almost all solution-mined caverns are tested on a regular basis to prove the absence of significant leaks. Various tightness tests are currently used. We focus on the simplest one: cavern pressure is built up to the testing figure, and pressure evolution as a function of time is recorded during several days. A significant pressure drop rate is a clear sign of poor tightness. In fact, together with a liquid leak, several phenomena may explain the pressure drop observed after a cavern has been rapidly pressurized. They must be identified and quantified to allow a correct interpretation of the test results. In some cases field data can be corrected for the effects of these phenomena, leading to a better estimation of the leak.

More precisely, one must distinguish between:

- The “apparent” leak, which is directly deduced from the observed pressure decrease, or $Q_{app} = -\beta V_c \dot{P}_i$, where $\dot{P}_i$ is the as-observed cavern pressure drop rate and βV_c is the cavern compressibility.
- The “corrected” leak, obtained when the effects of known and quantifiable mechanisms contributing to the apparent leak are taken into account.
- The “actual” leak

The objective of this paper is to identify those mechanisms that might contribute to the apparent leak and which, when properly accounted for, can potentially reduce the gap between the corrected leak and the actual leak.

IDENTIFICATION OF FACTORS CONTRIBUTING TO AN APPARENT LEAK

In addition to an actual leak, several phenomena contribute to brine pressure evolution in a closed cavern.

A first group of phenomena pre-exist the test: they include ground and air temperature variations, atmospheric pressure variations and Earth tides (their effects are relatively small; some of them are more or less periodic and their effects can be neutralized by analyzing 24-hour long increments of the test, see for instance Thiel 1993.) More significant are brine thermal expansion (caverns are created by circulating cold soft water in a deep salt formation where geothermal temperature is warm.) and pre-existing salt creep.

A second group consists of test-triggered phenomena. A comprehensive account of these phenomena is provided in Van Sambeek *et al*., 2005. They include transient brine permeation through the salt formation (pure rock salt permeability is exceedingly small; however salt-beds often contain a fair amount of insoluble rocks whose permeability is larger), additional dissolution (the amount of salt that can be dissolved in a given mass of water is a function of brine pressure; pressure build up in a closed cavern leads to additional dissolution; in the process the volume of cavern brine + dissolved salt decreases and pressure drops), brine cooling (a rapid pressure change leads to an instantaneous adiabatic warming of cavern brine) and transient salt creep.

BRINE THERMAL EXPANSION

The temperature of rock increases with depth, a typical value being T_R = 45°C at a depth of 1000 m, but caverns are leached out using soft water pumped from shallow aquifers whose temperature is smaller. Brine temperature at the end of leaching or T_i^o is close to the soft water temperature and significantly smaller than rock temperature (Van Sambeek *et al*., 2005). When the cavern remains idle, after leaching is completed, the initial temperature difference slowly resorbs with time, due to heat conduction in the rock mass and heat convection in the cavern. Appropriate heat-transfer equations can be written as follows:

$$\begin{aligned} &\frac{\partial T}{\partial t} = k_{salt}^{th} \Delta T \\ &\int_\Omega \rho_b C_b \dot{T}_i \; d\Omega = \int_{\partial\Omega} K_{salt}^{th} \partial T / \partial n \; da \\ &T_i(t) = T_{wall} \\ &T(t=0) = T_R \text{ and } T_i(t=0) = T_i^o \end{aligned} \tag{1}$$

The temperature in the rock mass is *T*; cavern brine temperature is T_i. The first equation holds inside the rock-salt mass (k_{salt}^{th} is the thermal diffusivity of salt, $k_{salt}^{th} \approx 3 \cdot 10^{-6}$ m²/s) ; the second equation is the boundary condition at cavern wall ($K_{salt}^{th} = k_{salt}^{th} \rho_{salt} C_{salt}$ is the thermal conductivity of rock-salt, K_{salt}^{th} = 6 W/m/°C is typical, and $\rho_b C_b$ = 4.8·10^6 J/m^3/°C is the volumetric heat capacity of brine). The third equation stipulates that rock temperature at cavern wall is equal to the average brine temperature in the cavern, a reasonable assumption as thermal convection stirs brine cavern effectively.
The exact temperature evolution can easily be predicted through numerical computations. Back-of-the envelope estimations can be reached simply: dimensional analysis proves that heat transfer in the rock mass is governed by one characteristic time, $t_c = R^2 / \pi k_{salt}^{th}$, where *R* is defined by $V_c = 4\pi R^3 / 3$, or $t_c(\text{years}) \approx V_c^{2/3}(\text{m}^2) / 800$. The second equation of (1) provides a second characteristic, or $t_c' = t_c / \chi$, $\chi = \rho_b C_b / \rho_{salt} C_{salt}$; however this second characteristic time is of the same order of

magnitude as t_c and must not be taken into account. In the case of a roughly spherical cavern, $2t_c$ is the time after which approximately 75% of the initial temperature difference has been resorbed. When V_c = 8,000 m^3, $2t_c \approx 1$ year. In a opened cavern, a temperature increase leads to thermal expansion and brine outflow at ground level, $Q = \alpha_b V_c \dot{T}_i$, where α_b is the brine thermal expansion coefficient, $\alpha_b \approx 4.4 \cdot 10^{-4} / °C$. In other words, when the initial temperature difference between rock mass temperature and brine temperature is $T_R - T_i^o$, the average brine volume increase rate during a $2t_c -$ long period would be:

$$Q_{average}(\text{in m}^3/\text{day}) = 0.75\ \alpha_b V_c (T_R - T_i^o)/2t_c = 3.6 \cdot 10^{-4} V_c^{1/3} (T_R - T_i^o),\ V_c \text{ in m}^3 \text{and } T_R - T_i^o \text{ in °C},$$

and the average pressure increase rate in a closed cavern is: $\dot{P}_i = Q_{average} / \beta V_c$, where β is the cavern compressibility factor. The actual pressure rate is much faster in a freshly washed out cavern, and slower at the end of the 2-t_c long period. It is faster in a smaller cavern. When cavern volume is V_c = 8,000 m^3, temperature initial gap is $T_R - T_{i0}$ = 20°C and the compressibility factor is $\beta = 4 \cdot 10^{-4}$/MPa, the average pressure build up rate in a closed cavern is 0.045 MPa/day.

Note that, in contrast with the four phenomena described below, brine thermal expansion makes the apparent leak smaller than the actual leak, i.e., thermal expansion hides some part of the actual leak. In the example above, the leak rate potentially hidden by thermal expansion is 50 m^3/year. As a general rule, brine warming is especially effective when the cavern is young (t/t_c is small), small and deep ($T_R - T_i^o$ is large).

ADDITIONAL DISSOLUTION

Together with transient creep, additional dissolution is the most significant "test-triggered" phenomenon. The amount of salt that can be dissolved in a given mass of water is an increasing function of brine pressure (and temperature): pressure build up in a closed cavern filled with saturated brine leads to additional dissolution; in the process, the volume of cavern brine + dissolved salt decreases, more room is provided to the cavern brine, and brine pressure drops. A new equilibrium is reached after several days. Magnitude of the pressure drop is easy to quantify; assessing additional dissolution kinetics is more difficult.

Consider a cavern filled with saturated brine. Cavern volume, brine volume, cavern brine pressure, saturated brine concentration and density are $V_c^0, V_b^0, P_i^0, c_{sat}^0, \rho_{sat}^0$, respectively (Brine concentration, or *c*, is the ratio between the salt mass and the water + salt mass in a given volume of brine). At the beginning of the process, $V_c^0 = V_b^0$. Then a volume of brine, or v^{inj}, is injected in the cavern and cavern pressure rapidly builds up to $P_i^0 + p_i^1$; p_i^1 is the (initial) testing pressure; it is related to the injected volume, or v^{inj}, through the cavern compressibility relation or $v_{inj} = \beta V_c^0 p_i^1$, $\beta = \beta_c + \beta_b$ where β_b is the brine compressibility factor (β_b = 2.7 10^{-4} /MPa is typical) and β_c is the cavern compressibility factor, a function of cavern shape and rock salt elastic properties (Young modulus and Poisson ratio), Bérest *et al.*, 1999.

In these new pressure conditions, brine is no more saturated. After some time (several days), the brine is saturated again and brine is said to have reached its "final state". Cavern pressure then is $P_i^0 + p_i^f$ and the other quantities are $V_c^f, V_b^f, c_{sat}^f, \rho_{sat}^f$. Brine concentration and density at saturation are functions of pressure variation:

$$c_{sat}^f - c_{sat}^0 = c_{sat}^0 \psi p_i^f$$
$$\rho_{sat}^f - \rho_{sat}^0 = \rho_{sat}^0 a_s p_i^f \quad (2)$$

The salt-mass balance equation and the brine-mass balance equation can be written:

$$V_b^f \rho_{sat}^f c_{sat}^f = V_b^0 \rho_{sat}^0 c_{sat}^0 + \rho_{salt} v_{salt}$$
$$V_b^f \rho_{sat}^f = V_b^0 \rho_{sat}^0 + \rho_{sat} v_{sat} \quad (3)$$

where $\rho_{sat} v_{sat}$ is the mass of dissolved salt. These equations lead to (4) and (5):

$$v_{salt} = V_b^0 \frac{\rho_{sat}^0}{\rho_{salt}} \frac{c_{sat}^0}{1 - c_{sat}^0} \psi p_i^f = \lambda V_b^0 p_i^f \quad (4)$$

Where $c_{sat}^o = 0.2655$, $\rho_{sat}^0 = 1,200$ kg/m^3 , $\rho_{salt} = 2160$ kg/m^3 and $\psi = 2.6 \cdot 10^{-4}$/MPa lead to $\lambda = 0.52 \cdot 10^{-4}$/MPa. (These figures are after ATG Manual, 1985; they hold for a solution of pure water and pure NaCl; when an actual cavern is considered, these figures must be considered as indicative rather than exact).

$$V_b^f - V_b^0 = V_b^0 \left(\frac{\rho_{salt}}{\rho_{sat}^0} \lambda - a_s \right) p_i^f \quad (5)$$

Now the change in cavern volume, or $V_c^f - V_c^0$, results from, on the one hand, the creation of new void, or v_{salt} , and, on the other hand, the cavern elastic volume increase or $\beta_c V_c^0 p_i^f$:

$$V_c^f - V_c^0 = v_{salt} + \beta_c V_c^0 p_i^f = (\lambda V_b^0 + \beta_c V_c^0) p_i^f \quad (6)$$

We discuss here the simple case when brine is injected in a closed cavern to build up cavern pressure. Taking into account $V_c^0 = V_b^0$ and $V_c^f = V_b^f + v^{inj}$, Eq.(5) and Eq.(6) lead to:

$$v_{inj} = (\beta_c + a_s - \varpi) V_c^0 p_i^f \quad (7)$$

where $\varpi = \lambda \rho_{salt} / \rho_{sat}^0 - \lambda \approx 0.8\lambda$ = 0.416 10^{-4}/MPa and β_b is the brine compressibility factor (β_b = 2.7 10^{-4}/MPa is typical), which leads to the apparent leak caused by additional dissolution:

$$v_{leak}^{app} = (\beta_c + \beta_b) V_c^0 (p_i^1 - p_i^f) = \frac{a_s - \varpi - \beta_b}{a_s - \varpi + \beta_c} v^{inj}$$

where $a_s = 3.16 \cdot 10^{-4}$/MPa, $\beta_b = 2.7 \cdot 10^{-4}$/MPa, $\beta_c = 1.3 \cdot 10^{-4}$/MPa and

$$v_{leak}^{app} = 0.043 v_{inj}$$

For example, when the initial pressure build up is $p_i^1 = 5$ MPa in a $V_c^o = 50,000$ m^3 cavern such that $\beta V_c^o = 19.3$ m^3/MPa and when the injected volume is $v^{inj} = \beta V_c^o p_i^1 = 100$ m^3 , the apparent leak caused by dissolution is 4.3 m^3, and the final pressure after dissolution is complete is $p_i^f = 4.95$ MPa, or about a $p_i^1 - p_i^f = 0.05$ MPa pressure drop.

From the point of view of tightness test interpretation, a key question is : how long does the saturation process lasts. The answer is difficult. Brine saturation occurs through multiple processes, including diffusion inside the boundary layer at the cavern wall and convection and diffusion through the cavern. The whole process is difficult, perhaps impossible, to compute exactly; its duration is likely to depend on cavern size and age. Based on a few field data we propose to characterize the dissolution process using the following differential equations:

$$\frac{\partial c}{\partial t} = \frac{1}{t^{diss}} \left(c_{sat}^f - c \right)$$
$$\frac{\partial \rho}{\partial t} = \rho_{sat}^0 \beta_b \frac{\partial P}{\partial t} + \frac{1}{t^{diss}} \left(\rho_{sat}^f - \rho \right)$$

where t_c^{diss} is a constant of empirical origin, t_c^{diss} = 2.5 days typically.

ADIABATIC PRESSURE INCREASE IN A CAVERN

When pressure is rapidly increased in a fluid-filled cavern, the cavern fluid experiences an instantaneous temperature increase ("adiabatic compression"). This temperature increase is a fraction of a degree Celsius. Even though small, this temperature may be significant because it is achieved during a short period of time: it is followed by brine cooling and a subsequent pressure drop in a closed cavern. This transient pressure drop is quite fast during a couple of days and may lead to misinterpretation of a tightness test.
The first law of thermodynamics states that any change in the internal energy of a body is the sum of the amount of heat received by the body and the amount of work performed on the body. In other words the second equation of (1) must be more exactly re-written as:

$$\int_\Omega \left[\rho_b C_b \dot{T}_i - \alpha_b T_i \dot{P}_i \right] d\Omega = \int_{\partial\Omega} K_{salt}^{th} \, \partial T / \partial n \; da$$

where T_i is brine (absolute) temperature and α_b is brine thermal expansion coefficient. During a slow process, the additional term (when compared to (1)) can be neglected. Conversely, when a rapid pressure change is considered, the surface integral in the right hand side of (1) can be neglected and the brine temperature change ϑ_i^1 resulting from a rapid pressure change by p_i^1 is:

$$\vartheta_i^1(°C) = \left(\frac{\alpha_b T_i}{\rho_b C_b} \right) p_i^1 \text{ (MPa)}$$

In the case of a brine-filled cavern, C_b = 3,800 J/kg-°C, $\alpha_b = 4.4 \cdot 10^{-4}$/°C, $T_i \approx 300$K, $\rho_b = 1200$ kg/m^3 and the instantaneous temperature change is $\vartheta_i^1(°C) = 2.9 \cdot 10^{-2} \, p_i^1$ (MPa) or $\vartheta_i^1 = 0.15°C$ when $p_i^1 = 5$ MPa (or 700 psi). The temperature change is larger when the cavern is filled with hydrocarbons. This temperature change is followed by a cooling process which is governed by the equations described by (1). However testing duration is a few day long, a very short period when compared to the characteristic time t_c^{th}. In other words, temperature change during test duration is small and , in the case of spherical cavern, radius *R*, a closed form solution can be adopted:

$$\vartheta_i(t) - \vartheta_i(0) = -\frac{6\chi\alpha_b T_i}{\pi\rho_b C_b} \, p_i^1 \sqrt{t / t_c^{th}} \qquad\qquad t_c^{th} = R^2 / \pi k_{salt}^{th}$$

Taking χ = 4/9, $k_{salt}^{th} = 3 \cdot 10^{-6}$ m^2/s, $t_c^{th} = 1.23 \cdot R^2$ leads to:

$$\dot{\vartheta}_i(t) = -\frac{1.2 \cdot 10^{-2}}{R \text{ (m)}} \, p_i^1 \text{ (MPa)} / \sqrt{t \text{ (days)}}$$

or, when *R* = 12 m, $p_i^1 = 5$ MPa , $\dot{\vartheta}_i(t)$ = -0.005 °C/day after 1day and -0.0025 °C/day after 4 days.

BRINE PERMEATION THROUGH THE ROCK MASS

In the context of a tightness test, it is believed that leaks occur mainly through the cemented casing; however, leaks through the formation itself must be assessed. Pure rock salt exhibits a very low permeability. Permeability magnitudes as small as $K_{salt}^{hyd} = 10^{-22}$ to 10^{-20} m^2 are reported. Several authors believe that most of this (small) permeability is induced by cavern creation and operation. This generalization is likely different for bedded salt formations when the formation contains a fair amount of insoluble rocks (anhydrite or clay interbedded layers). Even in this case, steady-state leaks (i.e., when the cavern remains idle during a long period of time) are extremely small. However transient

leaks following a rapid pressure build-up may be significant. To allow simple estimations, we assume the following:

1. Darcy's law for fluid flow through porous media holds.
2. The hydraulic and mechanical processes are uncoupled.
3. Natural pore pressure before the test in the rock mass is assumed to be halmostatic (pore pressure equals the cavern pressure as it was before the test began). The incremental pore pressure increase is defined as $p(r,t) = P_{pore} - P_0$, where P_0 is the initial pore pressure (12 MPa at a 1000-m depth).

As a consequence, the incremental pore pressure evolution can be described by:

$$\frac{\partial p}{\partial t} = k_{salt}^{hyd} \Delta p$$
$$Q_{perm} = \int_{\partial\Omega} K_{salt}^{hyd} \partial p / \partial n \; da$$
$$p_i(t) = p_{wall}$$
$$p(\infty, t) = 0 \text{ and } p_i(t=0) = p_i^1$$

where K_{salt}^{hyd} (m^2) is the salt matrix intrinsic permeability, $k_{salt}^{hyd} = K_{salt}^{hyd} / \mu_b \beta' \phi$ is the hydraulic transmissivity, μ_b is the brine dynamic viscosity, β' is the rock matrix compressibility factor, ϕ is the rock mass porosity, Q_{perm} is the brine flow rate through the cavern wall. This system is very similar to system (1) which governs brine temperature evolution; however, in sharp contrast with system (1), the constants such as k_{salt}^{hyd}, K_{salt}^{hyd}, $\beta' or \; \phi$ are poorly known, making any quantitative assessment difficult. Here again we assume that test duration, which is a few days, is small when compared to the hydraulic characteristic time $t_c^{hyd} = \mu_b \phi \beta' R^2 / \pi k_{salt}^{hyd}$. Then in the simple case of a spherical cavern a closed form solution can be reached:

$$Q_{perm} = Q_{perm}^{ss} (1 + \sqrt{t_c^{hyd} / t})$$

where $Q_{perm}^{ss} = 4\pi R K_{salt}^{hyd} p_i^1 / \mu_b$ is the steady-state flow; it is especially significant when (a) the rock permeability is large (b) the cavern volume is small. However even in the somewhat extreme case when $V_c = 8{,}000 \; \mathrm{m}^3$ and $K_{salt}^{hyd} = 10^{-19} \; \mathrm{m}^2$, steady-state flow is small; when $p_i^1 = 5$ MPa and $\mu_b = 1.2 \cdot 10^{-3}$ Pa.s, $Q_{perm} = 2 \; \mathrm{m}^3$/year, a figure which is negligible in the context of a tightness test. However the transient flow rate is much faster. The duration of a tightness test always is smaller than t_c^{hyd} and

$$Q_{perm} \approx Q_{perm}^{ss} \sqrt{t_c^{hyd} / t} = 1.7 \cdot 10^{-2} \beta \; (\mathrm{MPa}^{-1}) \; V_c \; (\mathrm{m}^3) \; p_i^1 \; (\mathrm{MPa}) / R \; (\mathrm{m}) \cdot \sqrt{t \; (\mathrm{days})}$$

when $\phi = 10^{-2}$ and $\beta = \beta' = 4 \cdot 10^{-4}$ /MPa.

STEADY-STATE AND TRANSIENT CREEP

Introduction

At this step, a few comments on the mechanical behaviour of salt are helpful. No other rock has given rise to such a comprehensive set of lab experiments, motivated, to a large extent, by the specific needs of nuclear waste storage – see, for instance, the proceedings of the five Conferences on the Mechanical Behaviour of Salt (see References).

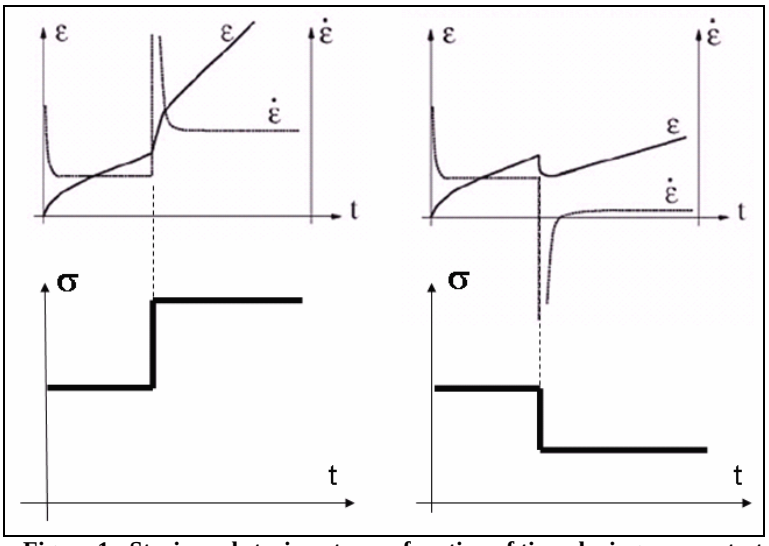

Figure 1 - Strain and strain rate as a function of time during a creep test.

Most experts agree on the main features of steady-state rock-salt behaviour:

a) In the long term, rock-salt flows even under very small deviatoric stresses
b) Creep rate is a highly non-linear function of applied deviatoric stress and temperature
c) Steady-state creep is reached after several weeks or months when a constant load is applied to a sample; it is characterized by a constant creep rate.
d) Transient creep is triggered by any rapid change in the applied stress. Transient creep is characterized by high initial rates (following a load increase) or by "reverse" initial rates (following a load decrease; "reverse creep" refers to a transient sample height increase following a decrease in the applied stress during an uniaxial test performed on a cylindrical sample) that slowly decrease or increase to reach steady-state creep (Fig.1).

Steady-state creep

Main features of steady-state creep are captured by the following simple model (Norton-Hoff power law):

$$\dot{\varepsilon}_{ss}^{ij} = A\exp\left(-\frac{Q}{RT}\right)\frac{1}{n+1}\frac{\partial}{\partial\sigma_{ij}}\left[\left(\sqrt{3J_2}\right)^{n+1}\right] \tag{8}$$

Where J_2 is the second invariant of the deviatoric stress tensor; A, n, Q/R are model parameters. Values of these parameters were collected by Brouard and Bérest, 1998: for 12 different salts, the constant n is in the range n = 3-6, illustrating the highly non-linear effect of the applied stress on the strain rate. Note that when a cavern (instead of a cylindrical sample) is considered, "transient" behaviour can be observed following a cavity pressure change – although Norton-Hoff constitutive behaviour includes no transient rheological behaviour. The reason is that after a pressure change, stress redistribute slowly inside the rock mass. Such a transient behaviour is called "geometrical".

Munson transient model

The Norton-Hoff model does not account for rheological transient creep. Better accounting for in situ observations require that transient creep be incorporated in the constitutive model. Munson and Dawson, 1984, suggested the following model:

$$\dot{\varepsilon}_{vp}^{ij} = F\dot{\varepsilon}_{ss}^{ij} \qquad \begin{aligned} F &= e^{\Delta(1-\varsigma/\varepsilon_t^*)^2} \quad \text{when} \quad \varsigma \le \varepsilon_t^* \\ F &= e^{-\delta(1-\varsigma/\varepsilon_t^*)^2} \quad \text{when} \quad \varsigma \ge \varepsilon_t^* \end{aligned} \tag{9}$$

$$\dot{\varsigma} = (F-1)\dot{\varepsilon}_{ss}, \quad \dot{\varepsilon}_{ss} = A\exp\left(-\frac{Q}{RT}\right)\left(\sqrt{3J_2}\right)^n$$

$$\varepsilon_t^* = K_0 e^{cT}\sigma^m \text{ and } \Delta = \alpha_w + \beta_w Log_{10}\sigma/\mu \quad , \delta=\delta_0$$

Note that this model accounts for "transient" creep, but predicts no "reverse creep" following a stress decrease.

A modified version of the Munson model

Munson *et al*. (1992) suggested a modified model taking into account the onset of "reverse creep" following a stress drop (i.e., a rapid pressure build up in a closed cavern). We propose a slightly modified version of this law that allows for simple computations:

$$F = 1-(1-\varsigma/\varepsilon_t^*)^p/(1-k)^p \text{ when } \varsigma > \varepsilon_t^*$$

And reverse creep appears when $\varsigma > k$. The model includes several new constants: a first group of constants, or $K_0, c, m, \alpha_w, \beta_w$ were inferred by Munson from lab tests performed on Gulf Coast salt. A second group of constants, or *k,p* were back-calculated from the results of in-situ tests. More research is still needed in this field, as salt transient behaviour play a very significant role in the interpretation of tightness test, as will be seen later. The approach suggested here, and the values of the parameters selected for numerical computations are still opened to discussion.

EXAMPLES

Pressure evolutions following the pressure build-up performed at the beginning of a tightness test were computed. The phenomena described above (brine warming, brine cooling following adiabatic compression, brine permeation, transient creep, additional dissolution) were taken into account. Several examples are described below (Figures 2 to 6). In all these examples, the actual liquid leak is assumed to be 164 m^3/year (1000 bbls/year). On each figure, in the right hand side rectangle, the effects contributing to pressure drop rate during a tightness test are listed; in most cases they include, together with the actual pressure drop rate (164 m^3/year) which appears in the lowest part of the rectangle, such effects as transient "reverse" creep, additional dissolution, transient permeation and brine cooling following adiabatic compression. Rather than the contribution of each phenomenon to the pressure evolution, or "$\dot{P} < 0$", the equivalent flow rates or "$Q = \beta V_c \dot{P}$" are indicated; β is the cavern compressibility factor and V_c is the cavern volume; $\beta = 4 \cdot 10^{-4}$ /MPa is assumed and several cavern volumes are considered. On the left hand side, in the upper part of the rectangle, phenomena contributing to pressure build-up rate, or "$\dot{P} > 0$" are listed; in most cases they include pre-existing creep and brine warming. The difference between factors contributing to pressure drop and factors contributing to pressure build up is the "apparent leak" which appears in the lower part of the left hand side rectangle. Comparison between the apparent leak and the actual leak is of special interest in the context of tightness test interpretation.

Example 1

This cavern is 600-m (2000 ft) deep and its volume is 14,137 m^3 (100,000 bbls). It was leached out in 150 days. One month after the cavern was washed out, a tightness test is performed: cavern pressure is built up through brine injection from 7.2 MPa (halmostatic pressure at cavern depth) to 10.2 MPa (testing pressure); brine injection lasts 2 hours. One day after the pressure was built up, the various transient phenomena triggered by pressure increase, which are displayed on the right hand side of Figure 2, still play a significant role; they are responsible for a 9 + 79 + 3 + 134 = 325 m^3/year equivalent leak rate. Brine warming is effective (as the test is performed a few weeks after leaching was completed) and hides a significant part of the leak. The actual leak rate (164 m^3/year) is slightly slower than the as-observed leak rate (208 m^3/year).

Two days later (day 3) the effects of the transient phenomena triggered by the test are considerably smaller; they are now responsible for a 4 + 33 + 3 + 11 = 51 m^3/year apparent leak rate. Brine warming is slightly slower than what it was on day 1. The as-measured leak rate (42 m^3/year) underestimates the actual leak rate (164 m^3/year): in this small and young cavern, the effects of brine warming are able to hide a large part of the actual leak (Figure 2).

Example 2

Same cavern as in Example 1 (cavern depth: 600 m, cavern volume: 14,000 m^3). The tightness test is performed 5 years (instead of 1 month) after the cavern was leached out. The main differences between Examples 1 and 2 are the following: (i) 5 years after cavern creation, in this relatively small cavern, brine warming is almost completed (ii) one day after pressure build-up, test-triggered (reverse) transient creep is slightly larger (243 m^3/year) than what it was in the case of Example 1, because cavern pressure has been kept constant during a much longer period (5 years instead of 1 month) before the test, allowing steady-state stress distribution to be reached in the rock mass. However transient creep rapidly changes its sign: 3 days after the test began, cavern shrinks again, as it did before the test (Figure 3).

Example 3

Same cavern as in Example 2 (the test is performed 5 years after the cavern was leached out). However the cavern is first pre-pressurized to 95% of the testing pressure; pressure is kept constant during 15 days; at the end of this period, cavern pressure is built up to its final figure (10.2 MPa) in two hours. As expected, “test-triggered” transient effects are much smaller than in Examples 1 and 2 (Figure 4).

Example 4

The cavern is the same as in Example 1, except for its depth which is 1200 m (4000 ft) instead of 600 m; accordingly, the pre-test pressure is 14.4 MPa and the testing pressure is 20.4 MPa (i.e., both pressures are twice larger than in Examples 1 and 2). Brine warming effects are larger than what they were (311 m^3/year instead of 208 m^3/year) because geothermal temperature at a 1200-m depth is warmer, resulting in larger temperature gap at the end of the leaching phase and faster brine warming; however, one day after the beginning of the test brine warming (“pre-existing heating”) is not able to hide the effects of transient “inverse” creep, which are must larger in a deeper cavern. Two days later (day 3) transient creep rate, which was 895 m^3/year, dramatically drops down. The apparent leak rate (33 m^3/year) underestimates the actual leak rate (164 m^3/year). This case clearly illustrates the significance of transient creep effects in a deep cavern. It must be kept in mind that the parameters describing transient creep are poorly known (Figure 5).

Example 5

Cavern depth is 1200 m (4000') and its volume is 525,583 m^3 ; the cavern was washed out in 700 days. The test is performed 5 years later. Before the test, a pre-pressurization period was managed as in Example 3 (however the testing pressure is 20.4 MPa). In this very large cavern, brine warming is still effective even 5 years after leaching was completed. Test-triggered effects are more or less proportional to cavern volume: although a pre-pressurization period is observed, these effects are still much larger than the effects of the actual leak, as the actual leak is assumed in these examples to be independent from cavern size. In a very large cavern, this testing procedure (pressure decrease observation) cannot be recommended as the apparent leak may be very different from the actual leak. Even a long testing period (several weeks) is not able to significantly improve test accuracy (Figure 6).

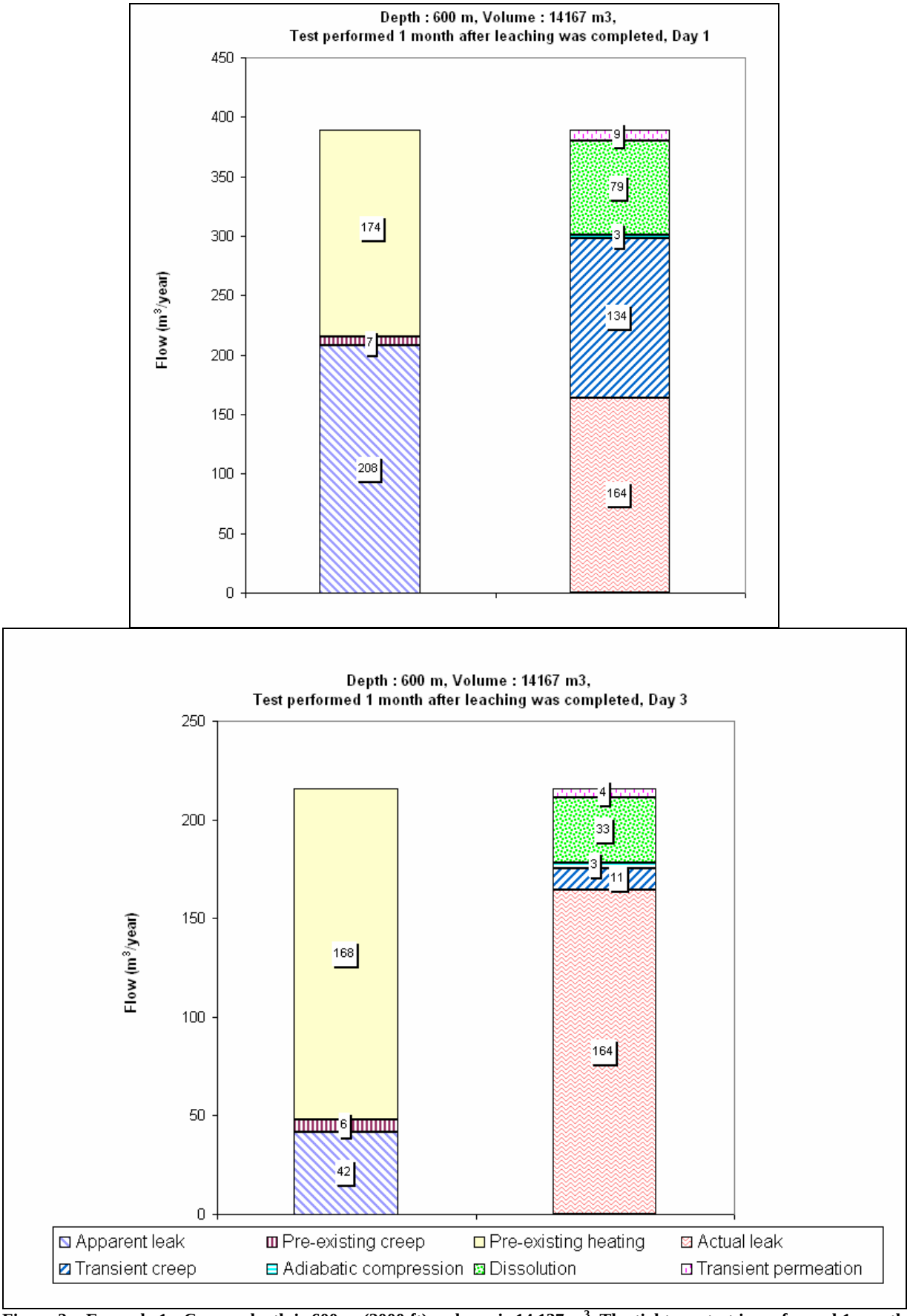

Figure 2 – Example 1 - Cavern depth is 600 m (2000 ft), volume is 14,137 m^3. The tightness test is performed 1 month after the cavern was leached out. Flows after one day (top) and Flows after 3 days (bottom).

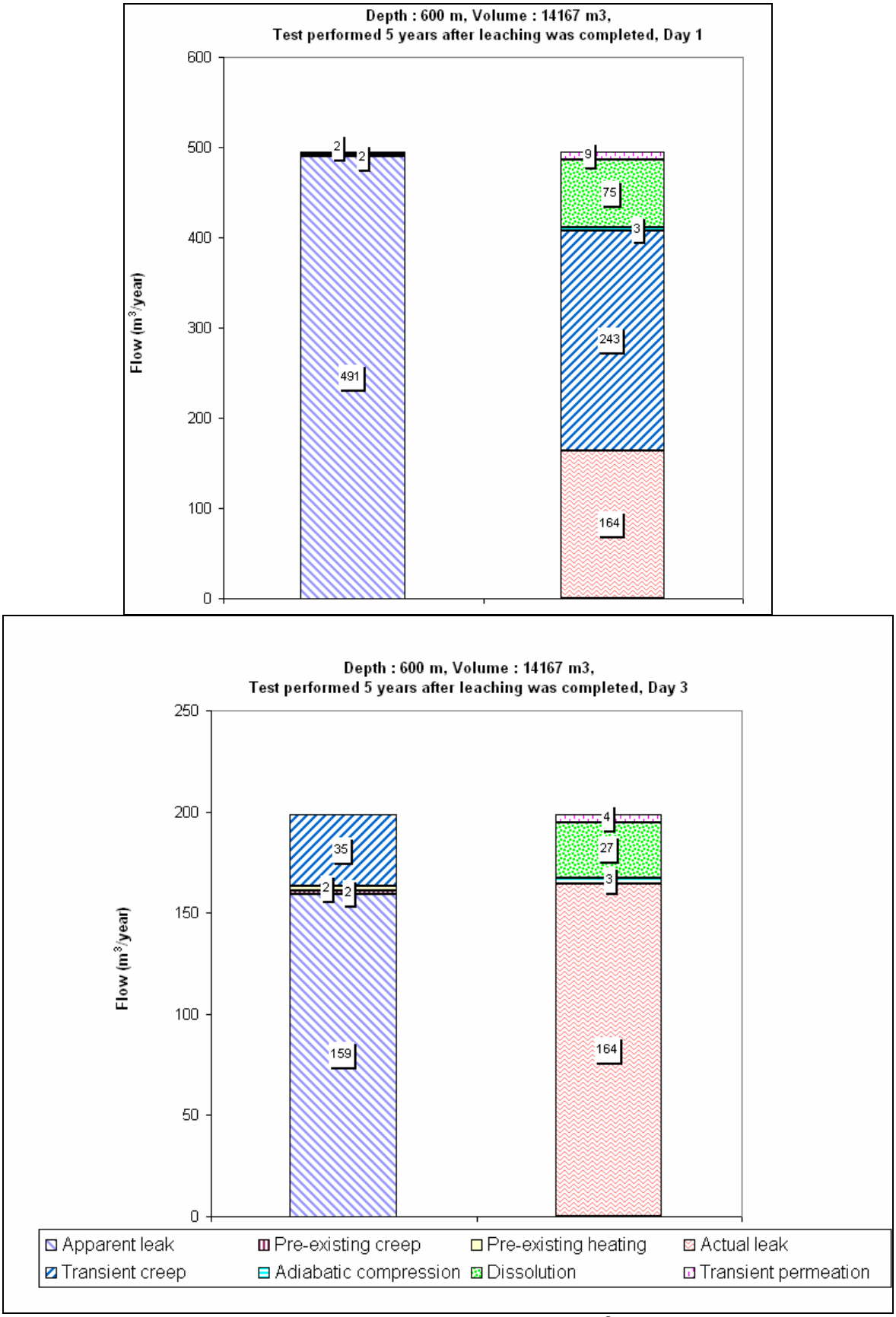

Figure 3 – Example 2 - Cavern depth is 600 m (2000 ft), volume is 14,137 m^3. The tightness test is performed 5 years after the cavern was leached out. . Flows after one day (top) and Flows after 3 days (bottom).

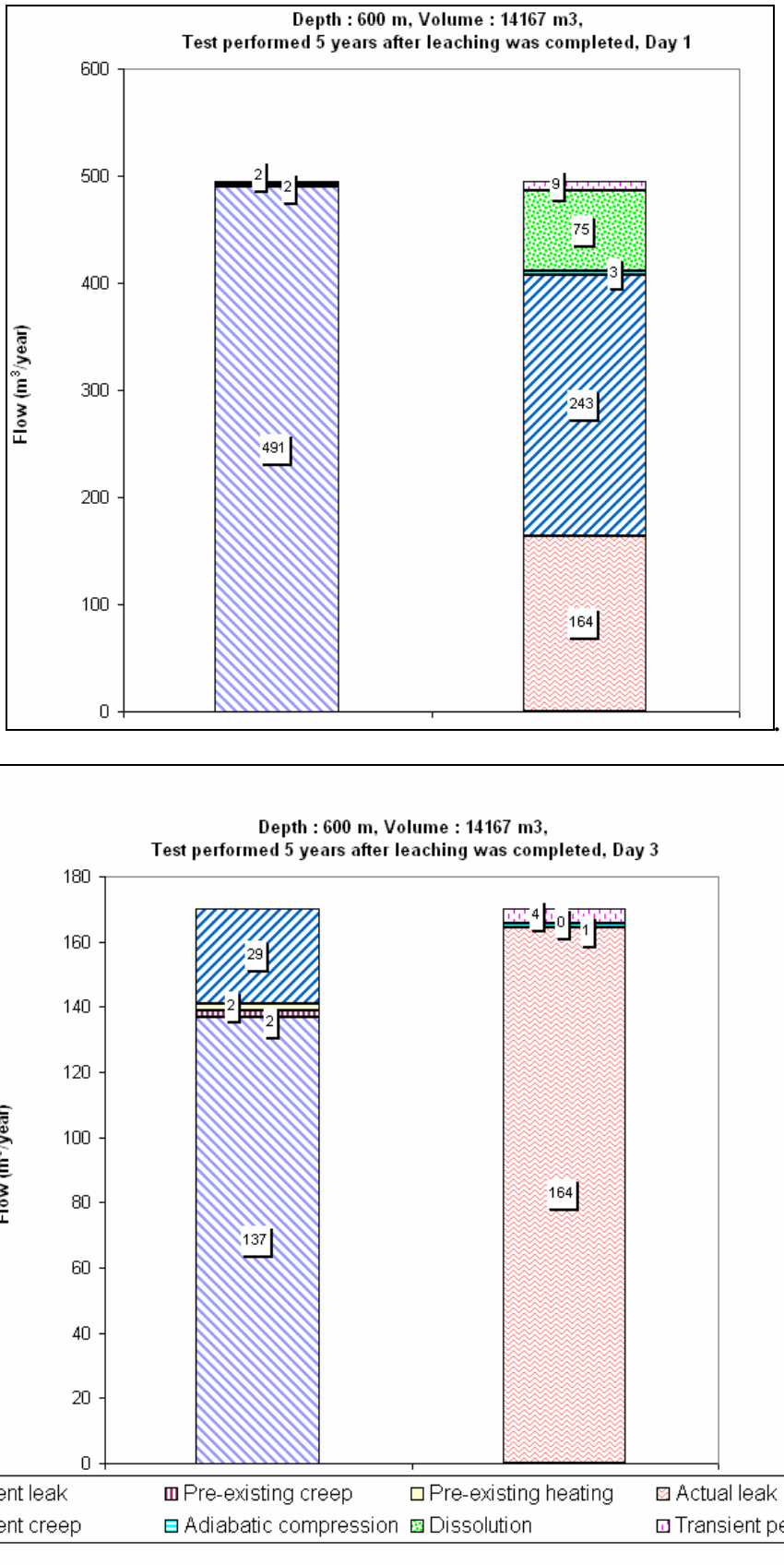

Figure 4 – Example 3 - Cavern depth is 600 m (2000 ft), volume is 14,137 m^3. The tightness test is performed 5 years after the cavern was leached out. The cavern has been pre-pressurized. after one day (top) and flows after 3 days (bottom).

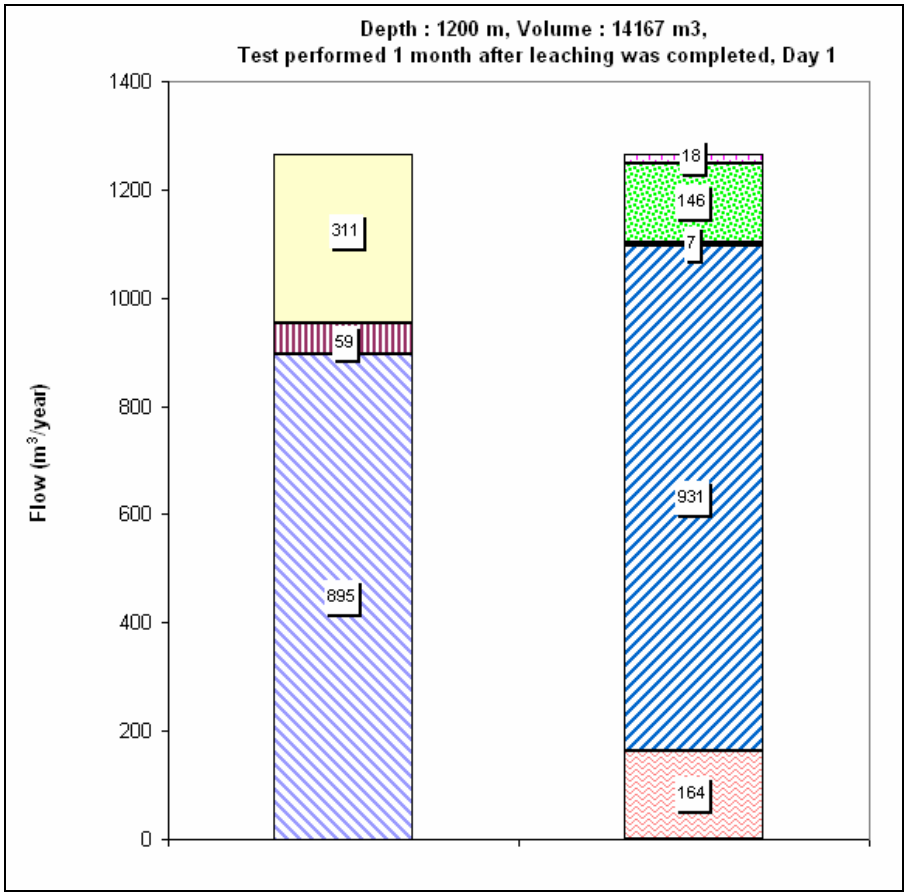

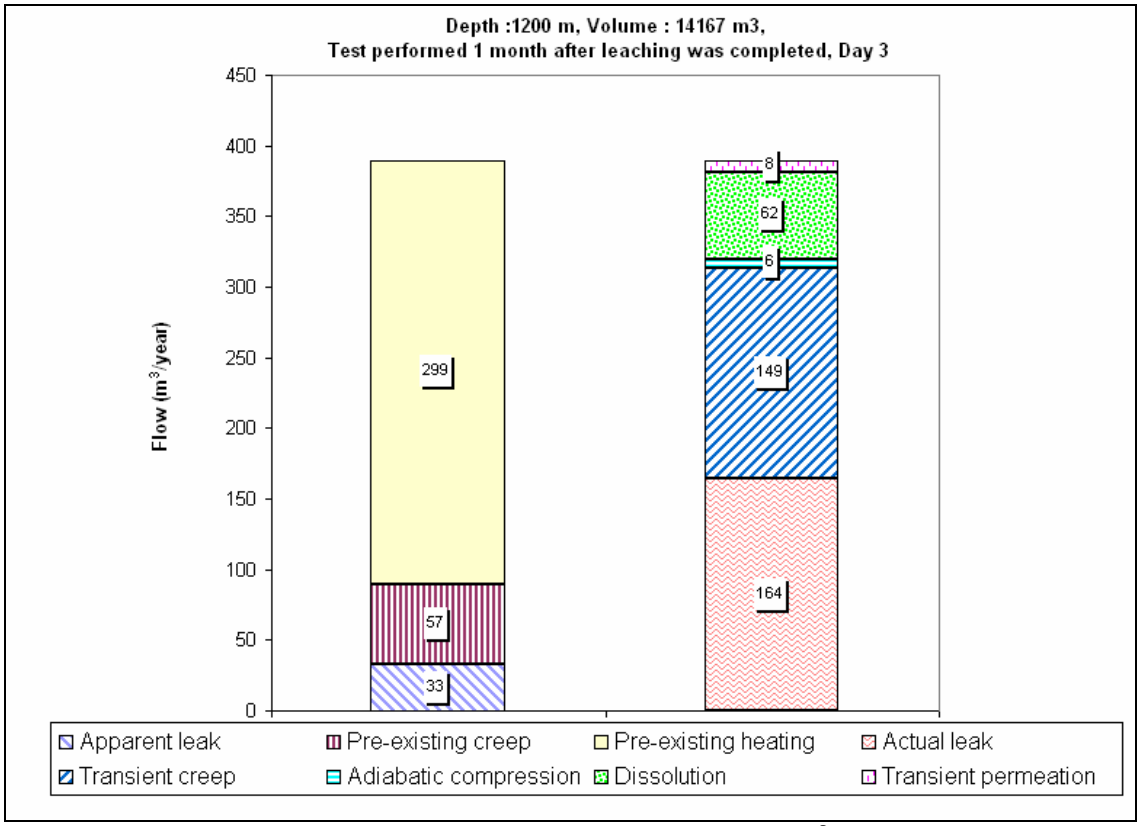

Figure 5 - Example 4 - Cavern depth is 1200 m (4000 ft), volume is 14,137 m^3. The tightness test is performed 1 month after the cavern was leached out. Flows after one day (top) and flows after 3 days (bottom).

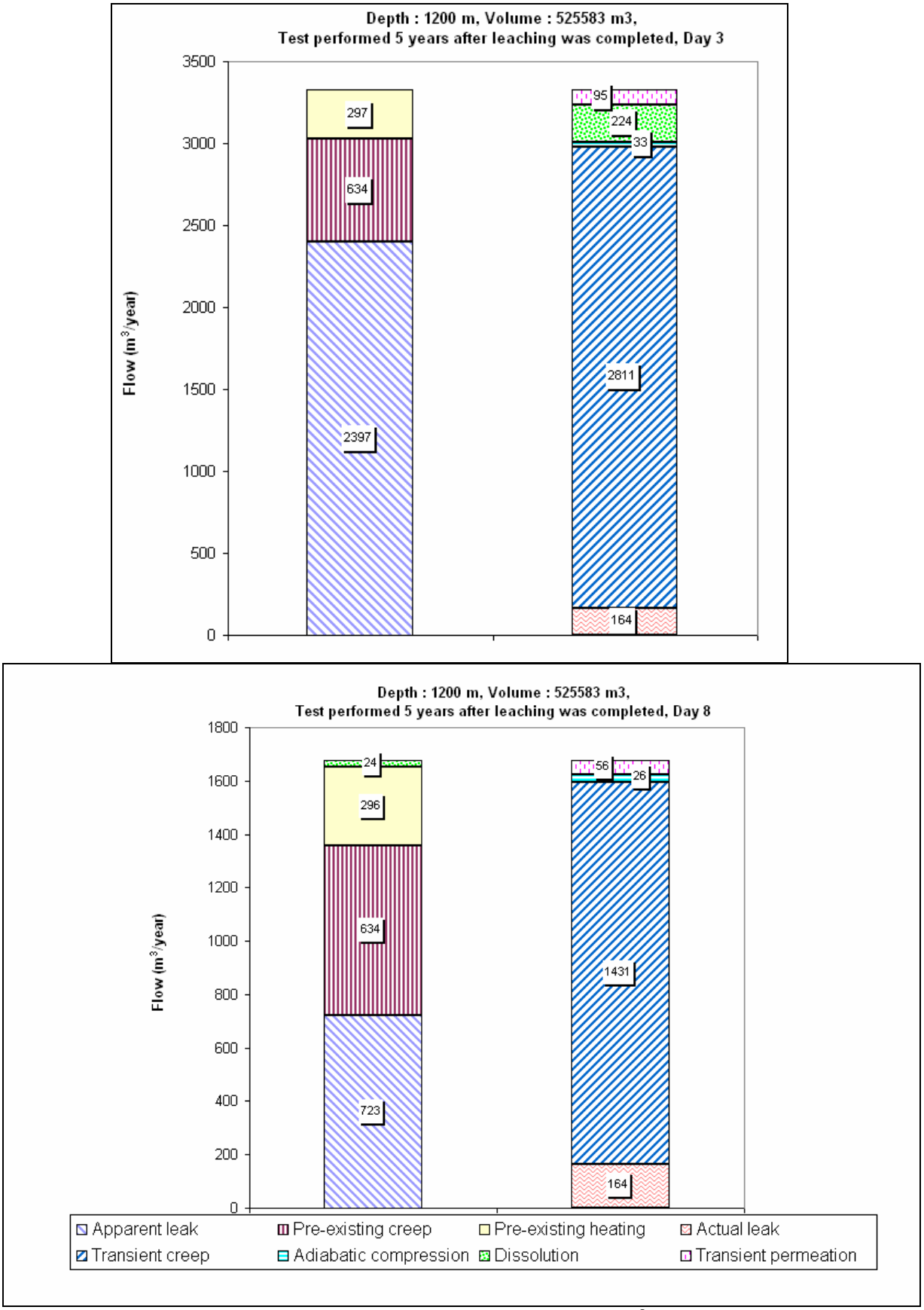

Figure 6 - Example 5 - Cavern depth is 1200 m (4000 ft), volume is 525,583 m^3. The tightness test is performed 5 years after the cavern was leached out. Flows after 3 days (top) and Flows after 8 days (bottom).

APPENDIX. A TEST ON THE EZ 53 CAVERN

We consider now an in situ test, first described by Hugout (1988), which allows to illustrate the various factors described above. The EZ53 cavern was leached out during the Spring of 1982 from the Etrez salt formation in France where Gaz de France operates natural gas storage caverns. It is a small cavern (7,500 +/500 m^3) and its average depth is H = 950-m. At this depth, rock temperature is T_R = 45°C. At the end of leaching phase, average cavern brine temperature was T_i^o = 26.5°C. Cavern was kept idle after the leaching phase was completed. Cavern brine slowly warms up; temperature was recorded from time to time. As explained above, brine warming results in brine outflow from the open well-head. The cavern brine temperature was 35.22°C on September 8, 1982 (day 94 after leaching ended) and 36.09°C on day 123. The average temperature increase rate during this period was 0.032°C/day, a figure consistent with back-of-the-envelope calculations (see above) and a Q = 100 litres/day brine outflow rate could be expected.

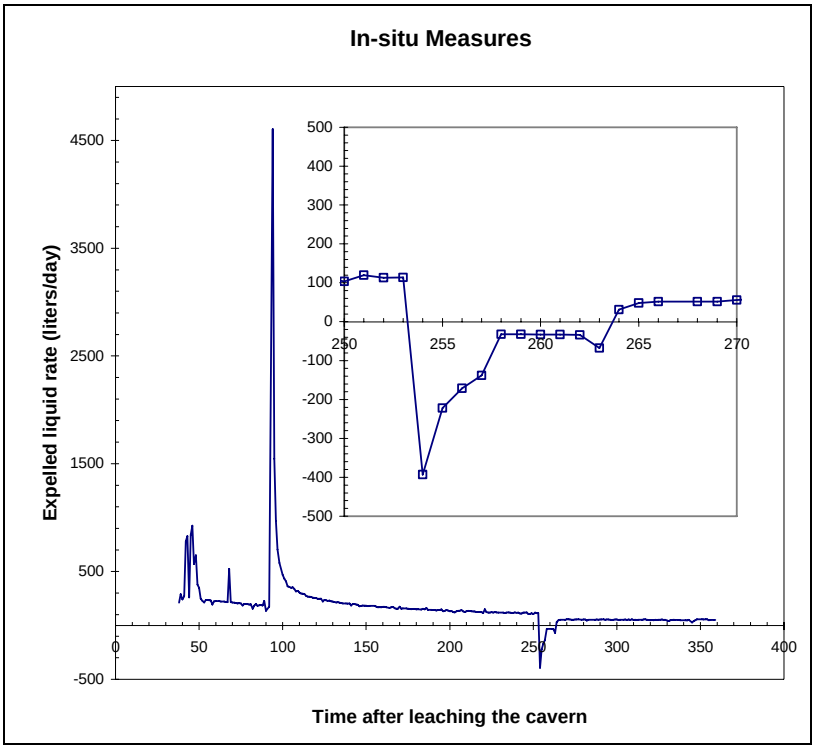

Figure 7 - Liquid outflow rate (as observed).

In fact the actual rate was a little faster (Fig.7); it is suspected that the difference was due to creep-induced cavern shrinkage. The annular space was filled with a light hydrocarbon (whose density was ρ_h = 850 kg/m^3). Hydrocarbon pressure at the well-head was approximately $p = g\ H\ (\rho_b - \rho_h)$ = 3.4 MPa (no pressure did exist at the brine-filled central tube well-head, which was opened to atmosphere, allowing brine to outflow from the cavern). On day 93, a valve was opened at the well-head to partially remove the hydrocarbon; the hydrocarbon pressure at the well head suddenly dropped to atmospheric pressure; the air/brine interface in the central string dropped by $h = p / g(\rho_b - \rho_h)$ = 290 m to balance the pressure drop in the annular space.

The hydrocarbon outflow rate was measured from day 93 to day 254 (Fig. 2). During a dozen of days, the hydrocarbon flow-rate is very fast, a clear sign of large transient effects in the cavern (the main effects are transient creep and additional crystallization). The flow more or less stabilizes after this initial period. It was larger than what the brine flow was before the pressure drop, a clear proof of the effect of cavern pressure on cavern creep rate (at a 950-m depth, the geostatic pressure is $P\infty$ = 21 MPa. Cavern pressure was P_i = 11.4 MPa before the pressure drop (brine density is ρ_b = 1200 kg/m^3) and P_i = 11.4 – 3.4 = 8 MPa after the pressure drop; in the idealized case of a spherical cavern, Norton-Hoff law, see Eq.(8), predicts that steady-state cavern volume loss is:

$$\dot{V}_c / V_c = -\frac{3}{2}\left(\frac{3}{2n}\right)^n \exp\left(-\frac{Q}{RT}\right)\left(P_\infty - P_i\right)^n$$

a simple relation which captures the non-linear influence of the cavity brine pressure, or P_i. The initial cavern pressure, or P_i = 11.4 MPa, was restored on day 253. This phase of the test is of special interest as it simulates the effect of a rapid cavern pressure increase. The annular space was closed at the well-head and the central tubing was filled with brine (Fig. 8). After this injection was completed, the brine level dropped in the central tubing (an effect of additional dissolution and transient cavern creep). Every 24 hours, brine was added to fill the central tubing. The daily amount of brine to be added gradually decreased, as transient effects slowly vanish. Eventually, 10 days after the first filling took place (day 263), brine was again expelled from the well-head and a constant brine-flow rate was observed, equivalent to 52 litres per day. The difference between the 100-litres per day outflow observed before the pressure drop (day 93) and the 52 litres per day observed a couple of weeks after cavern pressure was restored (day 270) is because brine thermal expansion is less and less active.
We focus now on transient phenomena, which are especially effective during the day 253 to 263 period. During this period brine was injected in the cavern (during days 253 to 261) or expelled from the cavern (during days 262 and 263). The total amount of brine injected (+) or withdrawn (-) during this period was carefully measured: -393-222-171-138-32-32-33-33-34-68+31+48 = -1077 litres (Note how rapidly injected brine flow-rate decreases at the beginning of this transient phase).

Thermal expansion and additional dissolution.

During the same 12-day period, the brine expelled flow due to brine warming should have been 52 litres/day (as it will be a few days later), or 624 litres during the 12-day period. As a whole, the cavern volume increase is 1077 + 624 = 1700 litres. A part of this volume increase is due to additional dissolution. At the beginning of this phase, brine was poured into the central tubing, resulting in an increase in cavern pressure by p = 3.4 MPa. The injection was rapid; no additional dissolution had time to take place during the injection. The initial amount of injected brine was $v_0^{inj} = \beta_c V_c^0 p + hS_t$, where S_t is the cross sectional area of the central string. In the following days, brine was injected in the cavern to keep cavern pressure constant or $p = p_i^f$. The volume of brine to be injected to balance the effect of additional dissolution is $v^{inj} - v_0^{inj} = (a_s - \varpi)V_c^0 p$, or 444 litres when $V_c^0 = 7500\ \mathrm{m}^3$ and $p = 3.4\ \mathrm{MPa}$. In other words, transient creep is responsible for a cavern volume increase by 1700 – 444 = 1350 litres (or a fraction of 1.8 10^{-4} of the overall volume). This volume increase is spread over a 10-day long period of time. After this period, cavern volume decreases again.

Transient creep

In order to analyze the effects of transient creep, numerical computations were performed. Cavern creation is simulated by a 3-month long linear decrease in cavern pressure from the geostatic figure to P_i = 11.4 MPa. Brine temperature at the end of the leaching phase is T_i^o = 26.5 °C. Pressure history is as during the actual test. Brine warming and additional dissolution or crystallization (following a pressure change) are taken into account. Brine volume change rate due to additional dissolution is assumed to vary as follows: $Q = v \cdot \exp\left(-t / t_c^{diss}\right) / t_c^{diss}$ where t_c^{diss} = 2.5 days. Transient behaviour is successively taken into account through the three above mentioned constitutive laws.

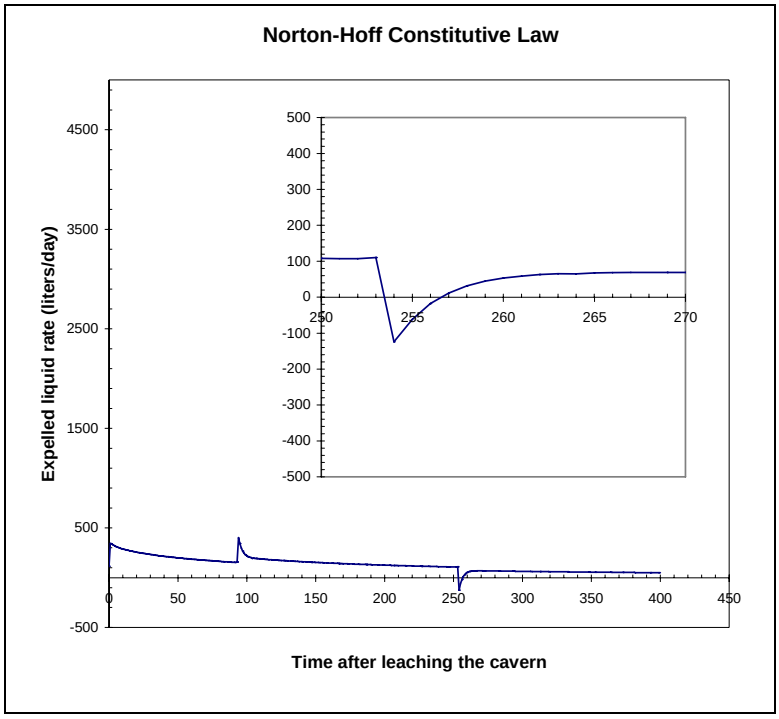

Figure 8 - Expelled liquid rate when Norton-Hoff constitutive law is considered.

This first model (Fig.8) takes into account brine thermal expansion, additional dissolution and steady-state creep (Norton-Hoff law). The parameters of the mechanical model were E = 25,000 MPa, ν = 0.25, A = 0.64 /MPa$^{3.1}$/year, n = 3.1, Q/R = 4100 K; these figures were obtained from laboratory tests performed on Etrez salt samples. The model is not able to describe the transient evolutions following pressure changes.

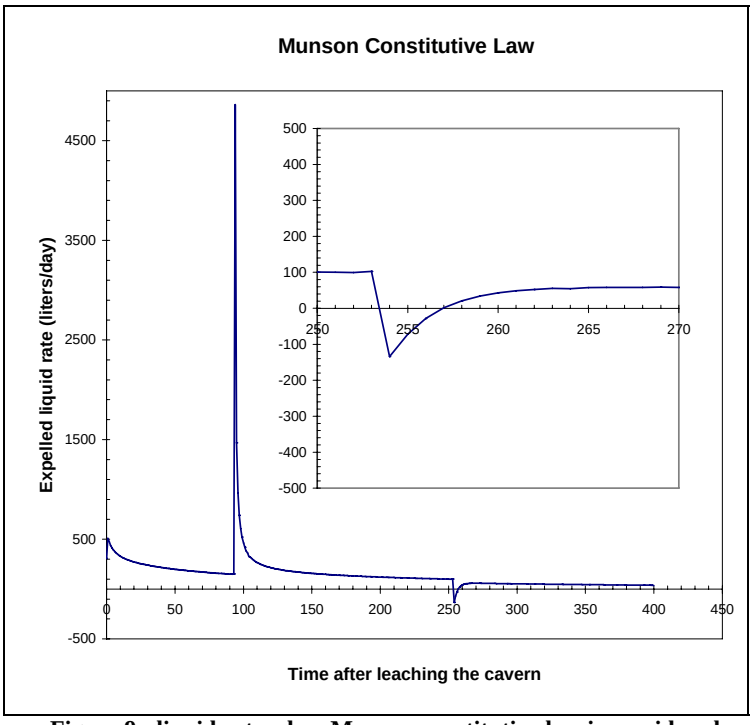

Figure 9 - liquid rate when Munson constitutive law is considered.

The second model (Fig.9) includes Munson-Dawson transient creep model. The model parameters were: m = 3.5, K_o = 6.7 10^{-11} /MPa$^{3.5}$, C = 0.0315, α_w = 10, β_w = 0, δ = 0.58. These figures were partly obtained from laboratory tests; figures published in the literature were also used. The effect of a

pressure drop is correctly captured. The “reverse” volume increase (negative brine outflow) observed after the day-253 pressure build-up is due to the effect of additional dissolution alone.

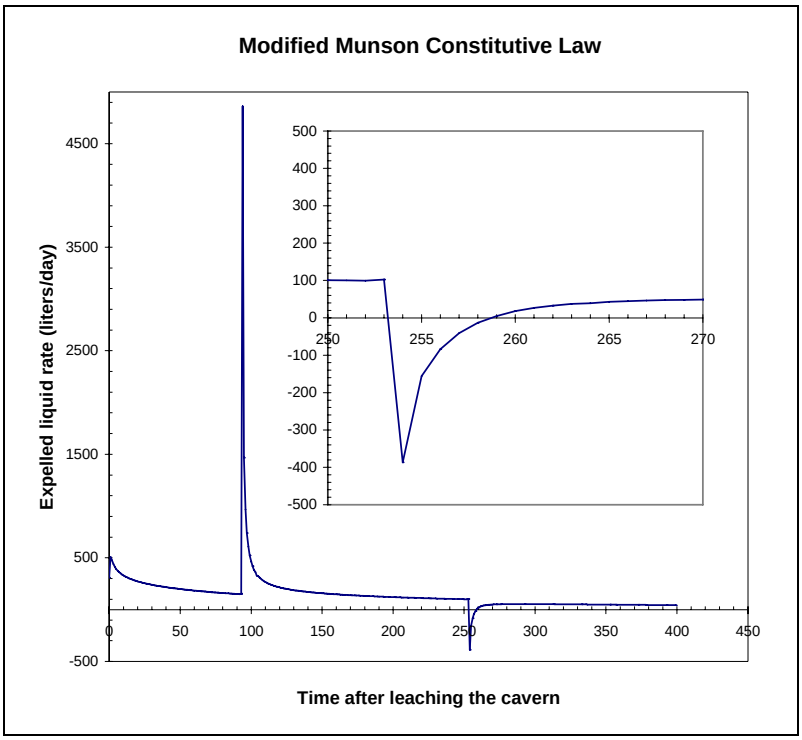

Figure 10 - Expelled liquid rate when Munson modified constitutive law is considered.

The third model (Fig.10) includes the modified Munson-Dawson model to reach a better description of transient “reverse” creep following a cavern pressure build-up. The model parameters are $p = 5$ and $k = 4$. These figures result partly from a (single) creep test performed on an Etrez salt sample; back-calculations also were used to reach a better agreement with in situ data.

REFERENCES

ATG Manual (1985). *Gas Transport and Distribution Handbook (Manuel pour le transport et la distribution du gaz. Titre XIII, Stockages Souterrains de Gaz)*. Association Technique de l'Industrie du Gaz en France, Paris, 333 pages (in French)

Aubertin M. and Hardy Jr R.H., editors, (1998). *Proc. 4th Conf. Mech. Beh. Salt*, Trans Tech. Pub., Clausthal-Zellerfeld, Germany.

Bérest P., Bergues J. and Brouard B. (1999) *Static and dynamic compressibility of deep underground caverns*. Int. J. Rock Mech. & Mining Sci., 36 :1031–1049.

Brouard B. and Bérest P. (1998). A classification of salt according to their creep properties. *Proc. SMRI Spring Meeting*, New Orleans, 18–38.

Cristescu N., Hardy R.H. Jr, Siminonescu O., editors, (1998). *Proc. 5th Conf. Mech. Beh. Salt*, Trans Tech. Pub., Clausthal-Zellerfeld, Germany.

Hardy Jr R.H. and Langer M., editors, (1984). *Proc. 1st Conf. Mech. Beh. Salt*, Trans Tech. Pub., Clausthal-Zellerfeld, Germany.

Hardy Jr R.H. and Langer M., editors, (1988). *Proc. 2nd Conf. Mech. Beh. Salt*, Trans Tech. Pub., Clausthal-Zellerfeld, Germany.

Hardy Jr R.H., Langer M., Bérest P., and Ghoreychi M., editors, (1996). *Proc. 3rd Conf. Mech. Beh. Salt*, Trans Tech. Pub., Clausthal-Zellerfeld, Germany.

Munson D.E. and Dawson P.R, (1984*).* *Salt Constitutive Modeling using Mechanism Maps*. Proc. 1st Conf. Mech. Beh. Salt, Trans Tech. Pub., Clausthal-Zellerfeld, Germany, pp.717-737.

Munson D.E., De Vries K.L., Fossum A.F. and Callahan G.D. (1996). *Extension of the Munson-Dawson model for treating stress drops in salt*. Proc. 3rd Conf. Mech. Beh. Salt, Trans Tech. Pub., Clausthal-Zellerfeld, Germany, pp.31-44.

Munson D.E. *Transient Analysis for the Multimechanism-Deformation Parameters of Several Domal Salts*. Proc. SMRI Fall Meeting, Washington DC, pp. 275-298, 1999.

Thiel W.R. (1993). *Precision Methods for Testing the Integrity of Solution Mined Underground Storage Caverns*. Proc. 7th Symp. on Salt, Kakihame H., Hardy H.R. Jr, Hoshi T., Toyokura K. eds., Elsevier, Vol. I, 377-383.

Van Sambeek L., Bérest P. and Brouard B (2005) *Improvements in mechanical integrity tests for solution-mined caverns used for mineral production or liquid-product storage*. SMRI Topical Report RSI-1799, 152 pages.